13th International Symposium on Turbulence and Shear Flow Phenomena (TSFP13)
Montreal, Canada, June 25–28, 2024

MACHINE-LEARNED SUB-GRID SCALE BACKSCATTER IN COARSE-GRID LES

Soju Maejima
Department of Aerospace Engineering
Tohoku University
6-6-01, Aramaki-aza-Aoba, Aoba-ku, Sendai, Miyagi, Japan
soju.maejima@dc.tohoku.ac.jp

Soshi Kawai
Department of Aerospace Engineering
Tohoku University
6-6-01, Aramaki-aza-Aoba, Aoba-ku, Sendai, Miyagi, Japan
kawai@tohoku.ac.jp

ABSTRACT

An unsupervised-machine-learning-based sub-grid scale (SGS) model for very coarse large-eddy simulations (vLES) is proposed. A prohibitive issue with vLES is that, because even the energy-containing eddies are not appropriately resolved, the resulting flowfield shows nonphysical features such as enlarged turbulent structures. Therefore, conventional SGS models which assume the resolved eddies to be physically accurate fail to make accurate predictions from the vLES flowfields. As a countermeasure to this issue, in addition to the typical supervised conditional GAN model, the proposed machine-learning pipeline has the unsupervised cycleGAN model preceding the conditional GAN model. The cycleGAN model converts the input vLES flowfield to be of filtered direct numerical simulation (DNS) quality so that the cycleGAN-produced filtered DNS data can be appropriately super-resolved by the supervised model. The predicted small-scale eddies are then extracted from the super-resolved flowfield to obtain the SGS stress components. The proposed unsupervised method is shown to be effective for accurate predictions of the mean streamwise velocity in vLES of a turbulent channel at the friction Reynolds number of $Re_\tau \approx 1000$, while the typical supervised-only methodology without the cycleGAN model shows discrepancies with the DNS profile, similar to other conventional SGS models. The budget analyses of the resolved Reynolds stresses revealed that the proposed SGS model predicts dominant SGS backscatter in the spanwise direction. The produced spanwise Reynolds stress is then redistributed to the wall-normal component of the Reynolds stress via the pressure term, where it gives rise to the increased Reynolds shear stress in the near-wall region. This kind of mechanism is not observed by the conventional SGS model. The results show that the prediction of SGS backscatter is crucial for accurate predictions in vLES and that the proposed unsupervised-learning-based pipeline is an effective method to achieve such predictions.

INTRODUCTION

Large-eddy simulation (LES) is considered to be a good compromise between the fidelity of the simulated turbulence and computational cost. To further reduce the computational requirements in LES, the development of a sub-grid scale (SGS) model for very coarse computational grids is desired. In regular LES, the SGS model is able to make accurate predictions of the SGS stress components from the well-resolved LES flowfields. However, in very coarse LES (vLES) considered in this study, the energy-containing eddies of turbulence are not fully resolved. The under-resolution of the energetic eddies causes the resolved turbulence structures to be nonphysically distorted and enlarged, resulting in a nonphysical energy increase near the cut-off wavelength. Therefore, existing SGS models based on known physics of turbulence fail to accurately predict the SGS components, resulting in inaccurate turbulence statistics.

The recent advances in machine learning have allowed various novel approaches to long-standing problems in fluid dynamics, including SGS modeling (Duraisamy (2021)). As machine learning is known to be successful at finding hidden relationships in data, it may be suitable for SGS modeling in vLES in which insights based on known physics of turbulence are not applicable.

An SGS model can be regarded as a function that takes the LES flowfields as the input and outputs the corresponding SGS stresses. A common method for training a machine learning model as an SGS model is to use the filtered DNS (fDNS) flowfields as the input and the corresponding SGS stresses as the output in the training data (supervised training). In other words, during training, the fDNS flowfields are used as substitutes for the LES flowfields which are the actual inputs to the model in the LES solver. The assumption with this method is that the LES flowfields closely resemble the fDNS flowfields used in training, that is, LES $\approx$ fDNS. While the assumption holds for well-resolved LES, it does not for vLES because the energetic eddies are not fully resolved by the coarse computational grid, that is, vLES $\neq$ fDNS. Therefore, the disagreement between the training data (fDNS) and the testing data (vLES) prevents the machine learning model from making ac-

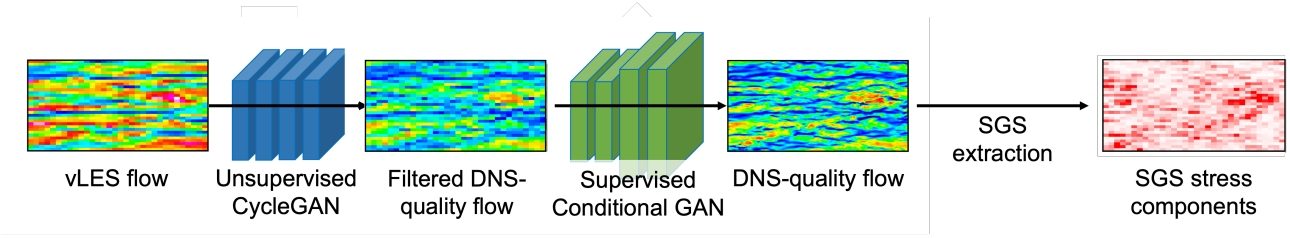

Figure 1: Schematic of the proposed unsupervised machine-learning pipeline.

curate predictions of SGS stresses. As a result, both the mean velocity and the Reynolds stresses are negatively affected leading to inaccurate prediction of turbulence. It is known (and shown in this work) that in vLES of wall turbulence, the insufficient prediction of the Reynolds shear stress leads to the over-prediction of the mean streamwise velocity.

In this work, we attempt to develop a machine-learning-based SGS model for vLES. The primary objective of this study is to obtain the accurate mean streamwise velocity profile of wall turbulence by introducing the appropriate SGS stresses and inducing the appropriate amount of Reynolds shear stress to the vLES flowfields. The proposed machine learning pipeline is constructed in such a way that allows accurate prediction of SGS stresses from vLES flowfields which is impossible with typical supervised-learning-based SGS modeling approaches. Both the *a priori* validation and the *a posteriori* test of the proposed SGS model are conducted using a fully-developed turbulent channel at a friction Reynolds number of $Re_\tau \approx 1000$.

METHODOLOGY

Machine learning pipeline

As mentioned above, a conventional supervisedly-trained machine learning model is unable to make accurate prediction of the SGS stresses from vLES flowfields. To alleviate this problem, we propose the unsupervised machine-learning pipeline as shown in Figure 1. In the proposed pipeline, the first model (blue in figure) transforms the input vLES flowfield to be statistically similar to an fDNS flowfield. The transformation allows the second model (green in figure) which is trained on fDNS data to perform accurate super-resolution and predict the SGS velocity components. In short, the two models together perform unsupervised super-resolution of the vLES flowfields. Finally, the SGS stress components are extracted from the super-resolved high-resolution flowfields and returned to the LES solver. To train the first vLES-to-fDNS model, supervised training cannot be utilized because the corresponding instantaneous fDNS flowfield for a given vLES flowfield does not exist. In this regard, we adopt the unsupervised cycle-consistency generative adversarial networks (cycleGAN) (Zhu *et al.* (2020)) which do not require pairs of the input and the expected output as the training data. The second super-resolution model is trained by a supervised conditional GAN Mirza & Osindero (2014) using fDNS flowfields and the corresponding DNS flowfields.

Computational setup

The proposed machine-learning-based SGS modeling methodology is trained and tested using a fully-developed turbulent channel at a friction Reynolds number of $Re_\tau \approx 1000$ and a bulk Mach number of $M_b \approx 0.1$. To train the machine learning models, the DNS and vLES of the turbulent channel are performed. The grid resolutions in wall units $(\Delta x^+, \Delta z^+)$ are approximately $(9.0, 4.5)$ and $(72, 36)$ for DNS and vLES, respectively. Both walls of the channel are non-slip walls, and the flow is periodic in the streamwise and spanwise directions. The second-order kinetic energy and entropy preserving scheme (Kuya *et al.* (2018)) is employed for the spatial discretization. For time integration, the third-order TVD Runge–Kutta method (Gottlieb & Shu (1998)) is employed. The selective mixed-scale (SMS) model (Lenormand *et al.* (2000)) is used as the SGS model in the vLES to generate the training data. In the *a posteriori* test, the same computational grid as the vLES is used.

We note that to stabilize the simulation in the *a posteriori* test, the predicted SGS stress $\tau_{ij,\mathrm{SGS}}$ is clipped according to the following equations:

$$\tau^{\mathrm{clip}}_{ij,\mathrm{SGS}} \equiv \begin{cases} \tau_{ij,\mathrm{SGS}} & \text{if } \mu_{\mathrm{eff}} > \mu_{\mathrm{clip}}, \\ \tau_{ij,\mathrm{SGS}} + \left(\frac{\mu_{\mathrm{clip}}}{\mu_{\mathrm{eff}}} - 1\right)\mu_{\mathrm{eff}} S_{ij} & \text{otherwise.} \end{cases}, \quad (1)$$

$$S_{ij} = \frac{\partial u_i}{\partial x_j} + \frac{\partial u_j}{\partial x_i} - \frac{2}{3}\frac{\partial u_k}{\partial x_k}\delta_{ij}, \; \mu_{\mathrm{eff}} \equiv \frac{\sum_{ij} \tau_{ij,\mathrm{SGS}} \frac{\partial u_i}{\partial x_j}}{\sum_{ij} S_{ij} \frac{\partial u_i}{\partial x_j}}. \quad (2)$$

Here, $\mu_{\mathrm{clip}} \equiv -2\mu_w$, where μ_w is the viscosity coefficient at the wall, is given as the simulation parameter.

VALIDATION

Here, to validate that the proposed machine-learning pipeline can learn to predict the SGS stresses, the pre-computed vLES flowfield is used as the input to the proposed machine-learning-based SGS model to test the prediction accuracy. The predicted mean SGS stress components normalized using the bulk density ρ_b and velocity u_b are shown in Figure 2. Compared to the typical supervised-only machine learning model without the unsupervised cycleGAN (dashed lines in the figure), the proposed unsupervised pipeline more accurately predicts the mean SGS stress components (solid lines in the figure). The over-prediction by the supervised-only model is the result of the differences between its fDNS training data and the vLES testing data. Because the vLES flowfield shows a non-physical increase near the cut-off wavelength compared to fDNS flowfields (vLES $\neq$ fDNS), super-resolution learned from fDNS over-predicts the strength of the small sub-grid scale eddies which leads to discrepancies in the extracted SGS stresses. The result suggests that the unsupervised cycleGAN model is effective for a more accurate SGS modeling in vLES.

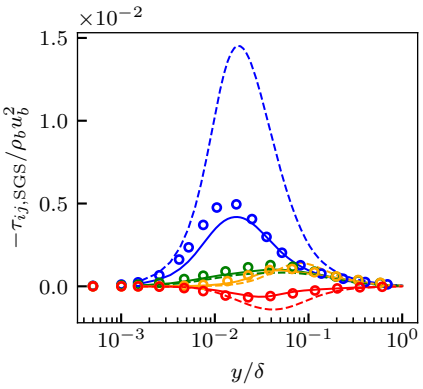

Figure 2: Profiles of predicted SGS stress components in *a priori* validation. Solid lines, proposed unsupervised pipeline; dashed lines, typical supervised-only model; circles, reference DNS. Blue, streamwise component; orange, wall-normal component; green, spanwise component; red, shear component.

RESULTS

Here, *a posteriori* test is performed by using the proposed unsupervised-machine-learning-based SGS model in the LES solver to assess its performance in LES simulations. Figure 3 shows the obtained instantaneous streamwise velocity distributions at $y^+ \approx 15$ with those of the vLES using the SMS model and the reference DNS for comparison. Compared to the DNS flowfield, the SMS model shows nonphysically enlarged streaky structures as mentioned in the introduction. In comparison, such enlarged structures are broken down by the proposed SGS model, creating finer turbulent structures which resemble more of the DNS flowfield.

Figure 4 shows the predicted mean streamwise velocity profiles and Reynolds shear stress profiles. The figure also shows the result for the typical supervised-only model (without the unsupervised cycleGAN model in Figure 1) for comparisons. The proposed model shows good agreement of the mean velocity with the reference profile, while the SMS model shows a significant over-prediction. Notably, the proposed model shows good agreement of the Reynolds shear stress in the buffer layer ($5 \lesssim y^+ \lesssim 30$) whereas the conventional SMS model predicts a significantly weaker Reynolds shear stress in this region, as mentioned in the introduction. From the shear stress balance of the equilibrium boundary layer, the near-wall rise in the Reynolds shear stress determines the amount of viscous shear stress, yielding the mean velocity profile. Therefore, the proposed SGS model with the correct near-wall Reynolds shear stress predicts the accurate mean velocity profile while the SMS model with its under-predicted Reynolds shear stress leads to the over-prediction of the mean velocity. These discrepancies predicted by the SMS model are also observed for the supervised-only model, showing the necessity of the unsupervised model in the proposed pipeline for accurate predictions. It is inferred that the small turbulent structures near the wall predicted by the proposed SGS model (observed in Figure 3) create the additional near-wall shear stress.

The obtained Reynolds normal stresses are shown in Figure 5. While there are only small differences between the proposed model and the SMS model for the streamwise component in the near-wall region, significant differences are observed for the wall-normal component. Considering that the Reynolds shear stress is the covariance between the streamwise and wall-normal components of the velocity in incompressible flows, the differences in the shear stress profiles observed in Figure 4 originate from the differences in the wall-

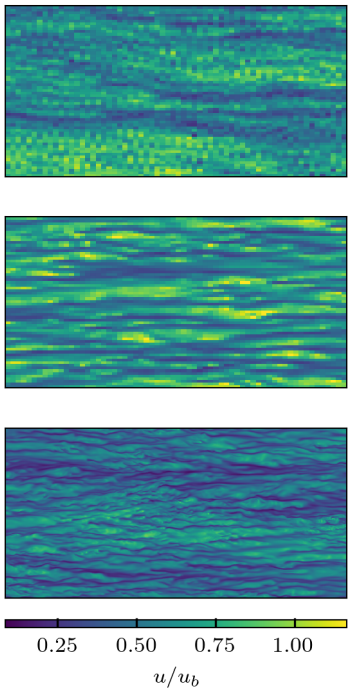

Figure 3: Instantaneous streamwise velocity distributions at $y^+ \approx 15$. Top, proposed unsupervised pipeline; middle, SMS model; bottom, reference DNS. Regions shown correspond to $(L_x^+, L_z^+) \approx (4600, 2300)$.

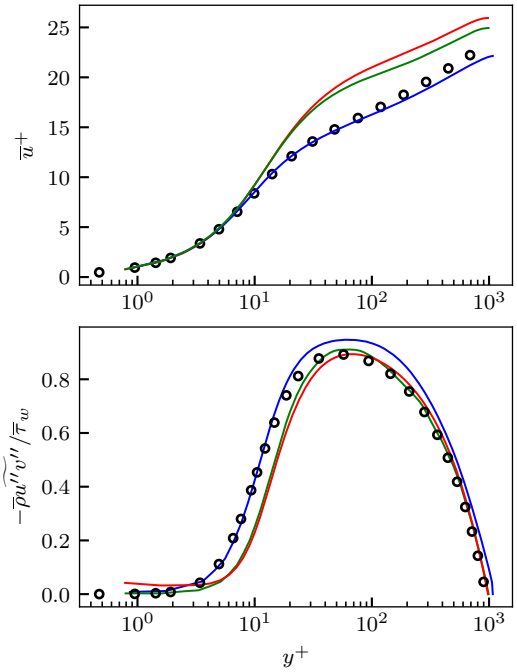

Figure 4: Obtained mean streamwise velocity (top) and shear stress (bottom). Blue lines, proposed model; green lines, typical supervised-only model; red lines, conventional SMS model; black circles, reference DNS.

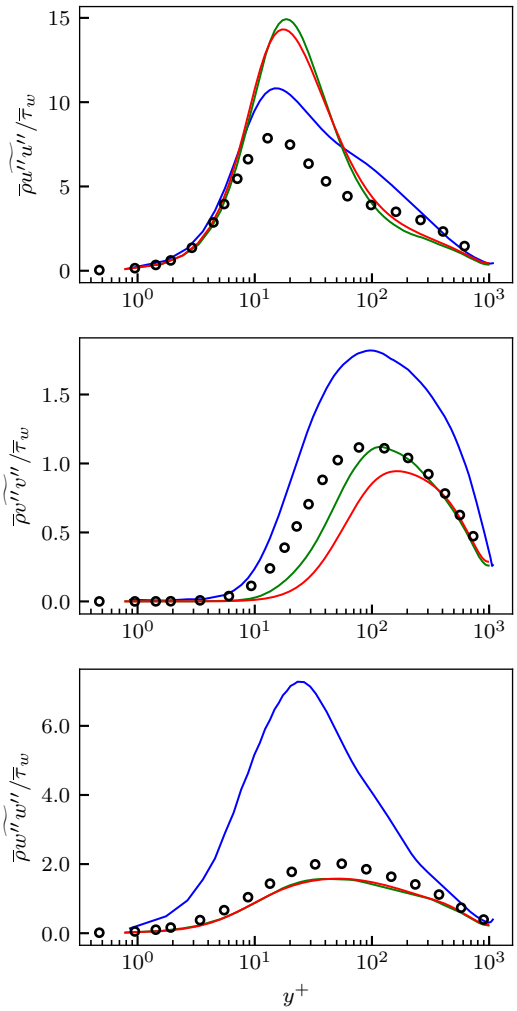

Figure 5: Obtained streamwise (top), wall-normal (middle), and spanwise (bottom) Reynolds stresses. Blue lines, proposed model; green lines, typical supervised-only model; red lines, conventional SMS model; black circles, reference DNS.

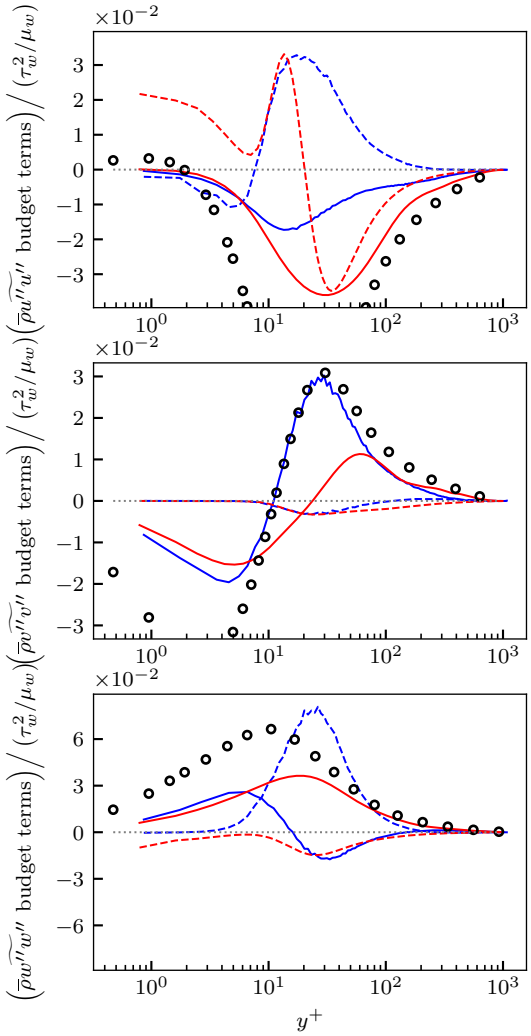

Figure 6: Streamwise (top), wall-normal (middle), and spanwise (bottom) components of Reynolds stress budget. Solid lines, pressure redistribution; dashed lines, SGS dissipation. Blue, proposed model; red, conventional SMS model. Black circles represent pressure redistribution of reference DNS. Horizontal dotted lines denote values of 0 in the vertical axes.

normal Reynolds stress. It is also notable that the spanwise stress is over-predicted by the proposed model. However, because the primary focus of this study is to obtain the accurate profile of the mean streamwise velocity as stated in the introduction, we do not consider this to be a failure of the proposed model.

To clarify how the different SGS models contribute to the predicted Reynolds stresses and the streamwise velocity, the budget analyses of the Reynolds normal stresses are conducted. A particular focus is placed on how the differences in the SGS stresses contribute to the increase in the wall-normal Reynolds stress, which leads to increased shear stress and better prediction of the mean streamwise velocity. As the supervised-only SGS model was observed to perform similarly to the SMS model, in the following, we will compare the proposed unsupervised-learning-based method and the SMS model.

The budget equation for each component of the resolved Reynolds normal stresses reads

$$\frac{\partial}{\partial t}\overline{\rho}\widetilde{u_i''u_i''} = C + P + T + D_v + D_{\mathrm{SGS}} + D_p, \tag{3}$$

where $C, P, T, D_v, D_{\mathrm{SGS}}$, and D_p denote the convection term, production term, transport terms, viscous dissipation term, SGS dissipation term, and pressure redistribution term, respectively. In this study, the SGS dissipation D_{SGS} and the pressure redistribution D_p are investigated in detail as the other terms show qualitatively similar tendencies across the different SGS models (not shown in this paper for brevity). Here,

$$D_{\mathrm{SGS}} = -\overline{\tau'_{ij,\mathrm{SGS}}\frac{\partial u_i''}{\partial x_j}},\ D_p = \overline{p'\frac{\partial u_i''}{\partial x_i}} \tag{4}$$

with the sum taken for the subscript j.

The profiles of the SGS dissipation and pressure redistribution terms for each directional component are shown in Figure 6. The SGS dissipation term D_{SGS} (dashed lines in figure) shows the contribution of the SGS stress to the total Reynolds normal stress in the turbulent channel, with the positive values signifying the production of Reynolds stress and negative values dissipation. In the wall-normal component, both the

proposed SGS model and the SMS model predict predominantly negative values and there are only minor differences in the profiles. In the spanwise component, on the other hand, the proposed SGS model predicts a primarily positive contribution of the SGS dissipation term whereas the SMS model predicts negative values throughout the channel. The positive contributions of this term represent the backscatter of turbulent kinetic energy, where the energy in the small unresolved eddies is transported to the larger resolved eddies. The energy backscatter in the spanwise direction explains the increased spanwise stress by the proposed SGS model observed in Figure 5. The SGS backscatter is also the cause of the energetic fine structures observed in the instantaneous flowfield (Figure 3).

The pressure redistribution term D_p of the three components satisfy $\sum_i p' \frac{\partial u_i''}{\partial x_i} = 0$ for incompressible flows and thus represents the transfer of Reynolds stress among the three directions; for example, from the streamwise component to the spanwise component. The profiles of the spanwise component reveal that, while the SMS model predicts a primarily positive contribution of this term, the proposed model predicts negative contributions in the buffer layer region ($5 \lesssim y^+ \lesssim 30$). As the negative values occur at around the same height as the peak of the SGS backscatter ($y^+ \approx 20 \sim 30$), it shows that some of the spanwise Reynolds stress created by the SGS backscatter is redistributed to the other two components. Correspondingly, the wall-normal component by the proposed model shows a positive contribution at the same wall distance. This suggests that the backscattered spanwise stress is redistributed to the wall-normal component, which leads to the increased wall-normal stress predicted by the proposed model. The increased wall-normal Reynolds stress then leads to the increase of the near-wall Reynolds shear stress and the better prediction of the mean streamwise velocity. In contrast, the SMS model predicts a weaker redistribution of Reynolds stress to the wall-normal component. Furthermore, the peak of the redistribution occurs further away from the wall at $y^+ \approx 70$. The resultant under-predicted near-wall shear stress leads to the over-prediction of the streamwise velocity. The results show that the strong redistribution predicted by the proposed unsupervised-machine-learning-based SGS model occurs because of the SGS backscatter in the spanwise direction, while the redistribution is significantly weaker in the SMS flowfield which does not predict the necessary spanwise SGS backscatter.

The above observations are compared with the mechanism of DNS discussed in detail by Lee & Moser (2019). In DNS, which resolves all relevant scales of turbulence, the streamwise Reynolds stress created by the near-wall production term P is first redistributed to the spanwise component. Then, the spanwise component is redistributed to the wall-normal component which gives rise to the near-wall shear stress. In the proposed SGS model, the predicted wall-normal Reynolds stress is produced mainly by the SGS backscatter in the spanwise direction. We note that because the goal of this study is to obtain accurate predictions of the mean streamwise velocity profile, the accurate prediction of the Reynolds shear stress is crucial. On the other hand, accurate predictions of the Reynolds normal stresses and their budget terms are out of the scope of this study. However, the above analyses have shown that while the proposed SGS model and DNS exhibit different turbulence mechanisms in the flowfields, they both lead to similar near-wall wall-normal stress. Therefore, the streamwise and wall-normal normal stresses together yield the accurate prediction of the shear stress, and the resulting streamwise velocities show good agreement.

Interestingly, a recent study on non-machine-learning-based SGS modeling for coarse-grid LES revealed that the successful SGS models for coarse grids also well predict the redistribution term of the wall-normal Reynolds stress budget (Inagaki & Kobayashi (2020)). This suggests that for very coarse grids that do not accurately resolve the energetic eddies, the accurate redistribution of the Reynolds stresses among the three directions is crucial to obtain the accurate mean velocity profile.

CONCLUDING REMARKS

In this study, we proposed an unsupervised machine-learning pipeline for sub-grid scale (SGS) modeling in coarse-grid large-eddy simulation (LES). The pipeline is composed of an unsupervisedly-trained cycleGAN model which converts the LES flowfields to filtered DNS quality and a supervisedly trained conditional GAN model which super-resolves the filtered DNS-quality flowfield to obtain the DNS-quality flowfields. The SGS stresses are extracted from the SGS scales of the resultant super-resolved flowfield. The *a priori* validation of the proposed approach shows that the unsupervised pipeline accurately predicts the SGS stresses for the turbulent channel, whereas the typical supervised-only approach shows large discrepancies with the reference profile. The *a posteriori* test performed using the proposed unsupervised-machine-learning-based SGS model in an LES simulation showed that the proposed SGS model predicts good agreements of the mean streamwise velocity with the reference DNS, whereas the conventional SMS model and the supervised-only model show significant over-predictions. The budget analyses of the Reynolds stresses revealed that the near-wall SGS backscatter in the spanwise direction predicted by the proposed SGS model gives rise to the increased near-wall spanwise Reynolds stress, which is redistributed to the wall-normal component to enable accurate predictions of the Reynolds shear stress and the resulting mean streamwise velocity profile. Such a mechanism was not observed for the conventional SMS, model, which suggests that the SGS backscatter is crucial for accurate predictions in coarse-grid LES.

ACKNOWLEDGEMENTS

This study was supported in part by JSPS KAKENHI Grant Number 22K18764. A part of the computations in this study was conducted by using the computational resources of a supercomputer Fugaku provided by the RIKEN Center for Computational Science through the HPCI System Research Project (Project ID: hp220034, hp230068, hp240083) and the Supercomputer system "AFI-NITY" at the Advanced Fluid Information Research Center, Institute of Fluid Science, Tohoku University.

REFERENCES

Duraisamy, Karthik 2021 Perspectives on machine learning-augmented reynolds-averaged and large eddy simulation models of turbulence. *Phys. Rev. Fluids* **6**, 050504.

Gottlieb, S. & Shu, C.-W. 1998 Total variation diminishing runge-kutta schemes. *Mathematics of computation of the American Mathematical Society* **67** (221), 73–85.

Inagaki, Kazuhiro & Kobayashi, Hiromichi 2020 Role of various scale-similarity models in stabilized mixed subgrid-scale model. *Physics of Fluids* **32** (7).

Kuya, Yuichi, Totani, Kosuke & Kawai, Soshi 2018 Kinetic energy and entropy preserving schemes for compressible flows by split convective forms. *Journal of Computational Physics* **375**, 823–853.

Lee, Myoungkyu & Moser, Robert D 2019 Spectral analysis of the budget equation in turbulent channel flows at high reynolds number. *Journal of Fluid Mechanics* **860**, 886–938.

Lenormand, E, Sagaut, P, Phuoc, L Ta & Comte, P 2000 Subgrid-scale models for large-eddy simulations of compressible wall bounded flows. *AIAA journal* **38** (8), 1340–1350.

Mirza, Mehdi & Osindero, Simon 2014 Conditional generative adversarial nets. *arXiv preprint arXiv:1411.1784* .

Zhu, Jun-Yan, Park, Taesung, Isola, Phillip & Efros, Alexei A. 2020 Unpaired image-to-image translation using cycle-consistent adversarial networks. *arXiv:1703.10593* .